Polymer Testing 120 (2023) 107947

Contents lists available at ScienceDirect

Polymer Testing

journal homepage: www.elsevier.com/locate/polytest

Study of the laser-material interaction for innovative hybrid structures: Thermo-mechanical characterization of polyethylene-based polymers

Mario Di Siena [a], Silvio Genna [a], Patrizia Moretti [a,*], Gennaro Salvatore Ponticelli [b], Simone Venettacci [b], Pietro Russo [c]

[a] Department of Enterprise Engineering, University of Rome Tor Vergata, Via del Politecnico 1, 00133, Rome, Italy
[b] Department of Engineering, University of Rome Niccolò Cusano, Via Don Carlo Gnocchi 3, 00166, Rome, Italy
[c] Institute for Polymers, Composites and Biomaterials, National Research Council, Via Campi Flegrei 34, 80078, Pozzuoli, Italy

ARTICLE INFO

Keywords:
Laser processing
Diode laser
Polyethylene
Hybrid structure
Thermo-mechanical analysis

ABSTRACT

This study deals with the experimental analysis of the effects of laser radiation on semi-crystalline polyethylene-based polymers. This paper has been developed as basis for future development of an innovative joining system, based on laser technology, to produce hybrid structures consisting of metal and polymer parts. Several process monitoring techniques, such as mechanical tensile test, thermogravimetric analysis (TGA), differential scanning calorimetry (DSC), flat-top cylinder indentation test (FIMEC) and infrared analysis (FTIR) have been used to evaluate the thermo-mechanical properties of the tested materials, with the aim to identify the technological process window for the joining process. The investigation, focused on two thermoplastic samples in high density polyethylene (HDPE) and polyethylene terephthalate (PET), aimed to investigate any structural changes caused by the laser irradiation of the polymer materials. Results showed no degradation for PET material and only a minor oxidation effect for black high-density polyethylene (HDPE) sample. The achievements of this study are of crucial importance for the identification and setting of the optimal irradiation parameters during laser joining operations, thus avoiding ineffective heating or excessive degradation of the material.

1. Introduction

The need to create ever lighter and more performing components has led to the development of hybrid structures [1], consisting of the coupling of different materials. Multi-materials of metal-polymer and metal-composite hybrid structures are highly demanded in several fields including land, air and sea transportation, infrastructure construction, and healthcare [2]. This coupling of materials makes it possible to exploit the different characteristics of the individual components, as in the metal-polymer case [3] while keeping a light structure with high mechanical characteristics [4]. Furthermore, the use of polymers can give to the structure a chemical stability [5], which is not possible to obtain with the lone metal alloy. In this context, the study and the development of new joining technologies for the construction of hybrid structures are of fundamental importance in many fields, especially for those where a high property/weight ratio is absolutely demanding. The adoption of composite hybrid structures in transportation industries represents a pivotal opportunity to reduce the product's weight without compromising structural performance [6]. This enables a significant reduction in fuel consumption for vehicles driven by internal combustion engines, as well as an increase in fuel efficiency for electric vehicles [7].

The automotive and aviation industries seek to replace metal components with thermoplastic composites to minimize vehicle weight [8]. Thermoplastic composites and high-performance thermoplastics are usually joined to metallic parts in complex assemblies, such as a vehicle body. Thus, hybrid metal-composite and metal-plastic systems are involved in many applications [9]. The mechanical properties, chemical composition and physical characteristics of dissimilar materials often make metal-polymer and metal-composite combinations relatively difficult. The main challenge to produce multi-materials of such hybrid structures is related to the lack of effective joining solutions [2,10]. Currently, the industrially available technologies on the market to create hybrid structures are conventional joining processes based on mechanical fastening [11] and adhesive bonding [12]. These solutions involve several issues and significant disadvantages, such as the need for part

* Corresponding author.
E-mail address: patrizia.moretti@uniroma2.it (P. Moretti).

https://doi.org/10.1016/j.polymertesting.2023.107947
Received 9 December 2022; Received in revised form 19 January 2023; Accepted 31 January 2023
Available online 1 February 2023

drilling, the use of fasteners for the mechanical joining, and, in general, are characterized by a high environmental impact for bonding. The adoption of inserted third parts (such as bolts or rivets) in mechanical fastening cause also overweighting [13] and increased costs [7] In this context, an innovative joining system, based on laser technology, will allow the elimination of mechanical fastening elements and adhesives, giving a strong push towards the automation of production, consequently ensuring a reduced environmental impact [2,7].

A key process in laser joining concerns the in-depth transmission of the laser radiation, that is up to the layer of the metal material to be joined, to ensure a good adhesion between the layers. In case of poor ability of the material to absorb and transmit radiation, the laser power can be increased, but it should not be too high in value, to avoid the risk of degrading the polymer [14]. Therefore, there is a temperature window between the melting temperature and the degradation temperature of the material, within which it is proper to process the polymer.

In this study, two different commercial polymers were chosen, i.e. black high-density polyethylene (black HDPE) and polyethylene terephthalate (PET), with the aim of comparing the response to laser radiation. The applied laser conditions have been selected to expect a possible degradation phenomenon in the first material (HDPE), and, instead, an invariability in the chemical-physical characteristics examined in the second one (PET).

A deep study has been devoted to the analysis of thermo-oxidative degradation of polyethylene (PE) in the temperature range 100–200 °C in air or other oxygen-rich atmospheres [15,16]. In this context, based on the results of the analysis of both the reflected, absorbed, and transmitted radiation rates and of the TGA, the optimal parameters of laser radiation were identified, such as wavelength, power, and laser beam focus. Downstream of the irradiation tests, the state of degradation of the polymeric material was evaluated in terms of transformation of the chemical structure by mechanical and thermal tests as well as spectroscopic analysis.

In literature, different characterization tests were performed to study the properties and degradation phenomena of polymers [17]. Methods and equipment include microscopy, chromatography, spectroscopy, thermal analysis and rheometry. Besides, some recently developed microextraction techniques have been useful to extract and determine trace concentration of released molecules during polymers' aging [18]. Moreover, mechanical properties were evaluated by performing FIMEC (Flat-top cylinder Indenter for MEchanical Characterization) test [19], based on the use of a flat cylinder which penetrates at a constant rate into the material to evaluate the local properties. As reported by Refs. [20,21], flat punch indenters are preferred when testing soft materials, to avoid puncturing the material and to ensure a large contact size/stiffness, to facilitate detecting the surface before too much sink-in occurs. The experimental trend of load-penetration curves, reported in Ref. [22], was modelled by an artificial neural network finding a good response for the proposed solution. Barletta et al. [23] performed flat indentation test verifying the superior performance of the photoluminescent HDPE, as result of the dispersion in the HDPE matrix of the mineral fillers, which increase the dimensional stability of the components and improve their deformation response. Other literature papers [24,25], applied FIMEC method in order to evaluate the local stiffness reduction of CFRP (carbon fibre reinforced polymer) plates, after different aging in water, demonstrating the ability of FIMEC test to discriminate between different surface conditions of the same material. Additional literature works reported flat-punch indentation tests of thermo-plastic materials [26,27], such as polymethyl methacrylate (PMMA), polycarbonate (PC), polystyrene (PS) and polyethylene terephthalate (PET), to evaluate the viscoelastic performance.

The calorimetric technique (DSC) is useful for understanding the phenomena that drive the crystallization dynamics both neat polymers and nanocomposites, i.e. PET/clay [28]. At the same time, the DSC technique is currently applied for analyzing various grades of polyethylene, making it possible to discover impurities or even mixture of high- and low-density PE in the sample [29]. The formation of low molecular weight compounds (such as monomers and oligomers, solvent residues, additives, products) constitutes one of the best indicators of the degradation of a commercial polymer. The detection of these released compounds, generated by chemical reactions, in turn activated by heating, allows to know the mechanism and degree of degradation of the polymer. It represents a key aspect, considering that these species can be released into the surrounding environment. In this context, FTIR is one of the most important techniques for the analysis of these released low molecular weight compounds [18], as already verified by Sharma et al. [30], which reported the evaluation of surface crystallinity of PET filaments from FTIR spectra.

In this context, the aim of this experimental research is to study the polymer's degradation due to laser radiation, evaluating the thermo-mechanical properties of the tested materials, both before and after being subjected to local melting during laser processing. This phenomenon can cause physical and chemical transformations, with the possibility of affecting the quality of the obtained junctions. Therefore, the present study identifies the optimal technological process window to be adopted for the realization of innovative hybrid polymer-metal composite structures.

2. Experimental

2.1. Materials

The specimens studied are cut from commercially available plates based on black high-density polyethylene (HDPE, RS code: 408–3829) and polyethylene terephthalate (PET, manufactured by NUDEC, S.A), whose characteristics are determined through the tests described in the following sections. The thickness of considered materials is 3.8 mm and 2.9 mm for HDPE and PET, respectively. In Table 1, the main properties of the HDPE and PET plates are reported.

2.2. Sample preparation

Polymer plates were cut using a Stepcraft D840 numerical control machine (CNC). The 828 burr, from MJ CNC Automation, equipped with two 0.8 mm cutting edges, a diameter of 2 mm, and a stem of 3.175 mm. The cutting speed, the depth of cut and the feed rate have been chosen in such a way as to guarantee the best quality of the lateral surface and at the same time the highest machining speed. The depth of cut was chosen according to the thickness of the material, specifically 4 mm (in case of single pass) and 3 mm (for two passes), for PET and HDPE respectively.

Table 2 shows the respective values of the cutting parameters adopted for PET and HDPE, while Fig. 1 shows the plates under processing. Please refer to Section 2.5, especially to Fig. 4, for more details about the geometry (i.e. dog-bone shape and dimensions) and parameters of the samples, prepared for the tensile tests.

2.3. Thermogravimetric analysis

ThermoGravimetric Analysis (TGA) of studied samples was carried out using a Perkin Elmer Pyris Diamond analyzer. The samples were heated from room temperature of 25 °C up to 800 °C at a heating rate of

Table 1
Main properties of HDPE and PET plates.

Property	HDPE	PET	Unit
Density	0.95	1.34	g/cm^3
Specific heat	1.1	1.1	J/gK
Tensile strength	25	59	MPa
Elongation	50	does not break	%
Flexural strength	175	86	MPa
Maximum operating temperature	+90	+60	°C

Table 2
Numerical control machine tool cutting parameters set for PET and HDPE.

Material	Cutting speed, rpm	Depth of cut, mm (Initial thickness, mm)	Rate, mm/min
HDPE	17,000	3 (3.8) – 2 passes	1200
PET	17,000	4 (2.9) – 1 pass	1000

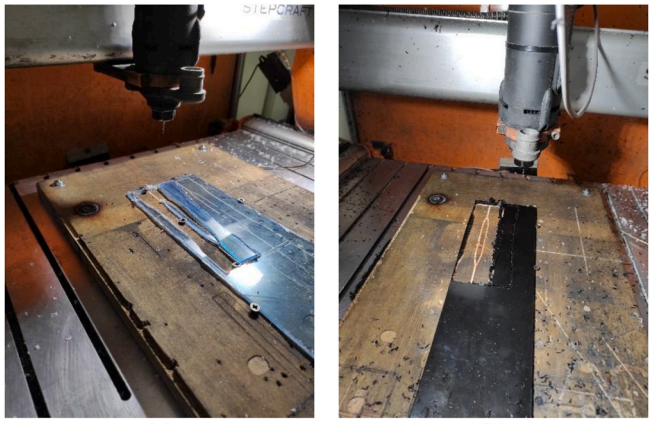

Fig. 1. PET (a) and HDPE (b) plates during CNC machining.

10 °C/min. The measurement was performed on 8–10 mg of sample placed in a ceramic crucible. For each sample, three replications were done. Nitrogen was used as carrier gas with a constant flow rate of 100 ml/min during the tests. Through the analysis of the TGA curves, is possible to determine the degradation temperature of the polymers, while the derived curve (DTG curve) allows to better highlight the weight variations of the sample. From these curves, three main temperatures can be identified: (i) the peak temperature of the DTG, corresponding to the inflection point of the TGA curve, which indicates the point of greatest rate of weight change (T_{DTG}); (ii) the "onset" temperature extrapolated according to ISO 11358-1 ($T_{on,E}$). This is the intersection point of the baseline of the initial mass and the tangent to the TGA curve at the point of maximum slope; (iii) the "onset" temperature according to ASTM E2550 (T_{on}). This represents the point in the TGA curve where a deflection from the baseline established prior to the thermal degradation event is first observed. The extrapolated onset temperature evaluation method is more easily reproducible [31]. In particular, the temperature $T_{on,E}$ will be referred to as the maximum temperature beyond which the degradation phenomenon definitively compromises the sample. In addition, temperatures $T_{1\%}$, and $T_{5\%}$, are reported, which represent the points of the TGA curve to which mass losses of 1% and 5% correspond respectively.

2.4. Laser treatment

A high energy efficiency and flat energy distribution IPG DRL 200 diode laser was used, characterized by a 975 nm (near infrared) wavelength source and a maximum power of 200 W, produced by IPG Photonics. A collimator, mounted at the end of the fibre optic cable, ensured a final spot of the radiation of about 6 mm. A beam expander (5 ×) gave the laser beam a diameter of about 30 mm and a FLIR A665sc thermal imaging camera allowed the temperature monitoring of the dog-bone shape specimens.

Fig. 2 reports a schematic view of the set-up configuration, while Fig. 3 presents the experimental setup. The laser irradiation tests were conducted under static conditions, i.e., without movement of the specimens, of which only the central zone was irradiated, as more clearly shown in Fig. 7 of Section 3.1. During the tests the working distance

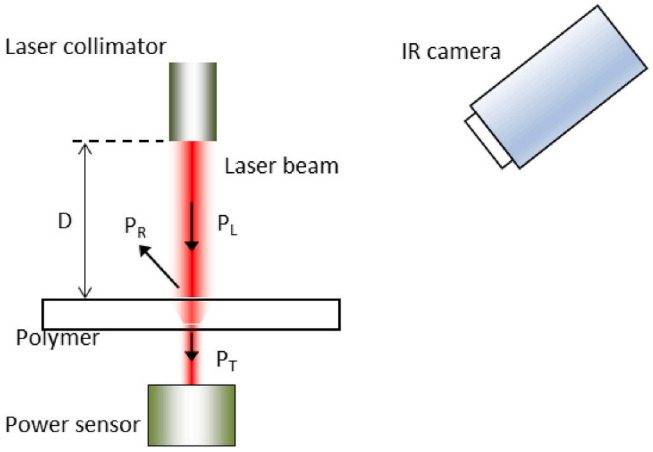

Fig. 2. Laser treatment scheme of the sample (PL, PR and PT indicate the Laser Power, the Reflected and the Transmitted Power respectively).

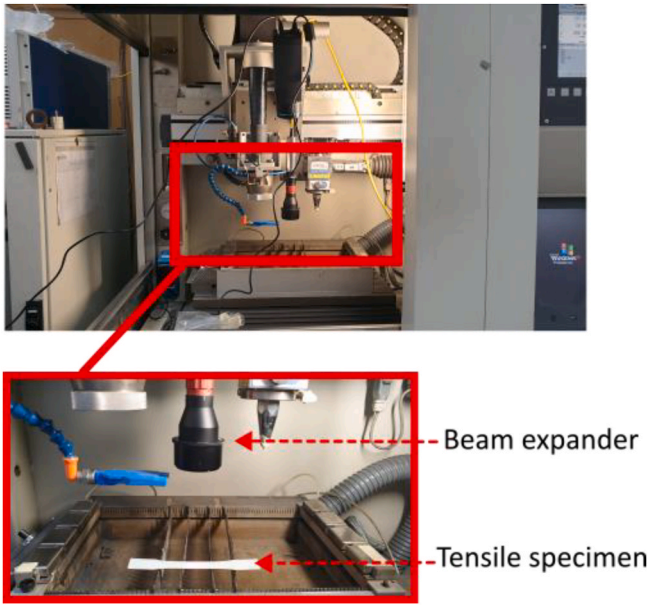

Fig. 3. Irradiation test setup.

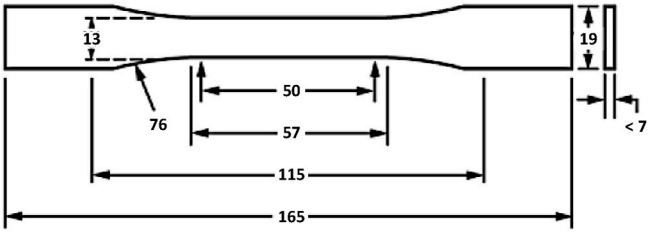

Fig. 4. Definition of the geometry and parameters of the samples, according to the standard ASTM D638. The dimensions are given in mm.

parameter, which refers to the vertical distance between the laser collimator and the top surface of the polymeric plates, was fixed at a distance (D) of 180 mm.

Table 3 shows the laser parameters experimentally measured with the OPHIRF150A-SH sensor, positioned on the opposite face of the sample, just below the plate and connected to the power meter Nova Display Assy by OPHIR. The energy parameters (i.e. treatment time and laser power) were selected after preliminary tests, in order to avoid

Table 3
Operating parameters of the laser used for the irradiation HDPE and PET.

Operating Parameters	HDPE	PET
Average Laser Power (W)	20	200
Laser runtime (s)	20	75
Maximum surface temperature measured (°C)	200	122

material degradation, and the power meter was manually reset before each measurement.

The high-energy beam penetrates a maximum thickness of a few millimeters into the semi-crystalline plastics and the distribution of heat within a polymer is dictated by the Lambert-Beer absorption law [32]. It is worth noting again that for the laser treatment, the samples adopted are those described in the following Section 2.5, regarding tensile tests, as they are also tested under tension to investigate any change due to the treatment itself.

The maximum temperature reached in the irradiated area was calculated using the FLIR ResearchIR software. The laser parameters were adjusted considering the thermo-gravimetric analysis, in such a way as to bring the temperature of the samples above the melting temperature and at the same time below the respective degradation temperatures.

2.5. Tensile test

For the tensile tests of polymeric materials, the ASTM D638 standard was considered as a reference for the definition of both the geometry of the samples (Type I) and other specifications as the crosshead speed and the distance between the clamps. Specifically, a crosshead speed equal to 5 mm/min and 500 mm/min, respectively for PET and HDPE, was chosen according to the stiffness of the polymer. Fig. 4 shows the geometry of the samples, while Table 3 reports the values selected for the parameters. Tensile tests were performed using the 50 kN MTS Insight electromechanical testing machine at room temperature. Mechanical parameters such as elastic modulus E, ultimate tensile strength UTS, stress at break σ_R, yield strength σ_S and strain at break $\mathcal{E}_R$ were recorded and processed. Three replicates for each material were performed. For each irradiated polymer, the percentage variation of the mechanical tensile properties, with respect to the untreated material, is calculated by applying Equation (1):

$$\Delta X\% = \left(\frac{X_{sample} - X_{reference}}{X_{reference}}\right)100 \quad (1)$$

2.6. Differential scanning calorimetry

Differential Scanning Calorimetry (DSC) tests were performed with the DSC Q2000 by TA Instruments. HDPE and PET samples, with a mass between 5 and 10 mg, were sealed in aluminium pans and heated from 20 °C to 200 °C [33,34] and from 20 °C to 280 °C [35,36] respectively (first thermal scans). The first scan was used to eliminate the thermal history of the material. Subsequently, the materials are cooled down to the starting temperature of 20 °C using a liquid nitrogen cooling device, adopting the same heating/cooling rate, fixed at 10 °C/min; finally, they are heated and cooled again to the same final temperatures (second thermal scans). Nitrogen flow rate was 20 ml/min.

The melting temperature (T_m), the crystallization temperature (T_c), the glass transition temperature (T_g), and the degree of crystallinity (X_c) were evaluated as fundamental parameters. For the calculation of the percentage of crystallinity, reference was made to Equation (2), where ΔH_m is the integral of the observed melting peak [37], ΔH_c is the heat of the crystallization during the heating phase (if present), and ΔH_0 is the thermodynamic fusion enthalpy of fully crystalline HDPE (i.e. 293 J/g [34]) or PET (i.e. 140 J/g [38]).

$$X_c = \left(\frac{\Delta H_m - \Delta H_c}{\Delta H_0}\right)100 \quad (2)$$

2.7. FIMEC indentation

FIMEC tests were carried out using the 5 kN MTS Insight 5 Universal Testing Machine, opportunely equipped with a 2.5 kN load cell and a fat cylindrical indenter, 1 mm in diameter, made of tungsten carbide. During the test, the applied load was acquired as a function of the penetration depth. Indentations were performed under quasi-static conditions (i.e. applying speed of 0.1 mm/min) to a maximum penetration depth of 0.5 mm. A 5 N pre-load was used to reduce the initial non-linearity of the curve due to the lack of perfect coplanarity between sample and indenter surfaces. On each sample schematized in Fig. 5, of dimension 5 × 1 cm, 10 indentations were performed at fixed positions 4 mm away from each other (named in the next sections as P1 to P10), obtaining load vs. penetration curves. Among the parameters that can be extracted by the obtained curves, the load value at fixed penetration depth and the slope in a given range of depths were evaluated. In particular, the slope of the linear trend is considered to be related to the mechanical stiffness of the indenter material. Indeed, FIMEC method allows the determination on a local scale of stiffness and yield stress, as obtained in standard tensile tests [23,24]. The FIMEC test was therefore conducted to investigate the mechanical performance of the samples as the distance from the source of the incident laser beam varies, along the 10 positions of indentation.

2.8. FTIR spectroscopy

To observe changes in a material caused by laser treatment, HDPE samples were characterized by Attenuated Total Reflectance Fourier Transform InfraRed spectroscopy (ATR FTIR) in the range from 4000 to 650 cm^{-1} with the aid of a Spectrum 100 FTIR spectrometer from PerkinElmer. A thin portion of the sample was extracted using a clean, sharp razor blade and pressed with a flat pressure tip. From each sample, three parallel spectral measurements were carried out, performed on different measurement points at sample surface. FTIR spectra were normalized using automatic baseline correction from the software Spectrum One by PerkinElmer.

FTIR spectroscopy allows to analyze the molecular structure of a material with the help of infrared radiation. In particular, when the binding energy and infrared energy are equivalent, the radiation is absorbed. The materials investigated were sampled in the lateral area (i.e. the portion of the specimens not affected by the laser) and in the central area (i.e. the one affected by the scanning).

3. Results and discussion

3.1. TGA analysis and thermal imaging analysis

The TGA curves are displayed from left to right for HDPE (a) and PET (b) samples in Fig. 6. Reference temperatures evaluated by processing these curves are collected in Table 4, together with the percentage of residual material.

A rapid degradation can be observed for both materials due to cleavage of the chemical bonding. Maximum weight loss was found in

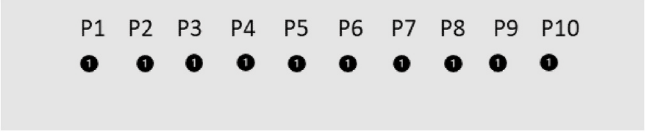

Fig. 5. Scheme of the sample subjected to FIMEC indentation test (real proportions).

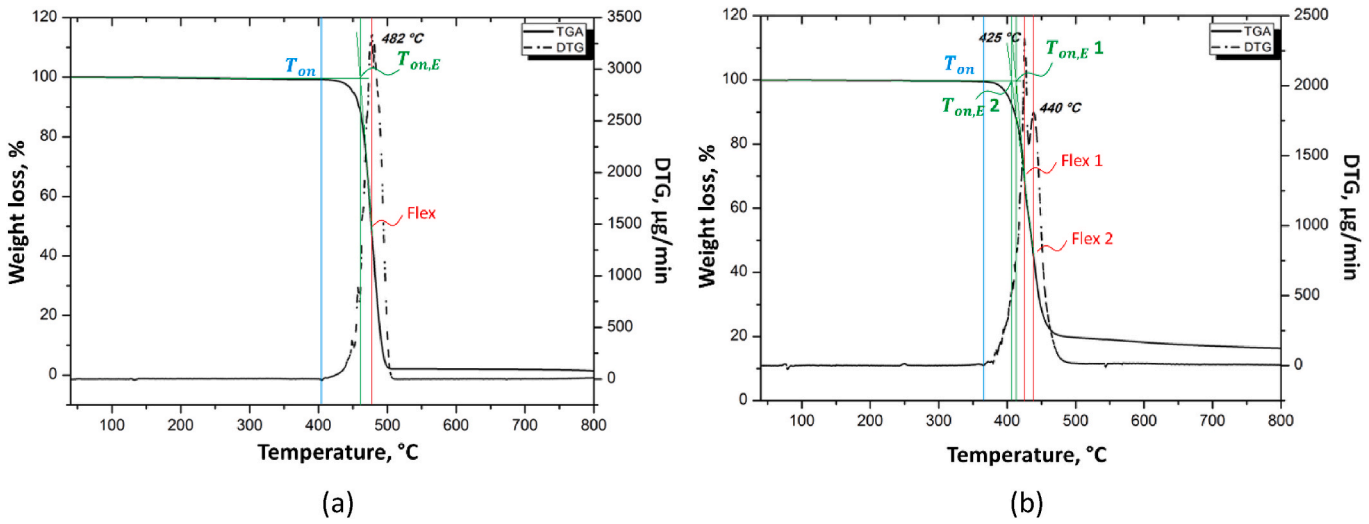

Fig. 6. TGA curve (solid line) and DTG (dotted line) of HDPE (a) and PET (b).

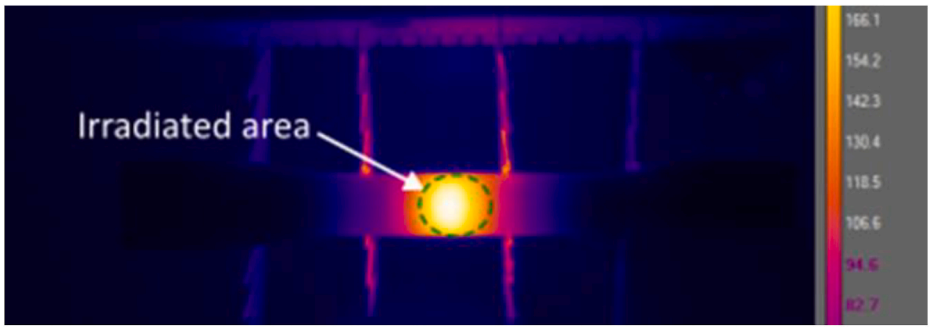

Fig. 7. Thermographic image acquired during the tests in the case of PET at 200 W.

Table 4
Thermal degradation properties of PET and HDPE evaluated by the TGA/DTG curves showed in Fig. 2.

Sample	T_{on}, °C	$T_{on,E}$, °C		T_{DTG}, °C		$T_{1\%}$, °C	$T_{5\%}$	Residue, %
HDPE	404	461		482		420	450	1.4
PET	366	405	414	425	440	382	400	16.8

the temperature range 420–500 °C and 380–480 °C for HDPE and PET, respectively. To further characterize the polymer samples, the extrapolated initial temperatures ($T_{on,E}$) was considered according to the ISO Standard, as they are more reproducible. $T_{on,E}$ denotes the temperature at which weight loss begins and corresponds to 461 °C for HDPE, while two values of $T_{on,E}$, corresponding to 405 °C and 414 °C, have been obtained for PET.

The first derivative curve is easily displayed by selecting the option under the MATH drop-down list of the software. In this case, the curve shows a peak centred at the temperature (T_{DTG}) corresponding to the maximum rate of weight change for the material examined as well as to the inflection point ("Flex") of the TG curve. The values of T_{DTG} evaluated for the materials examined were found to be 482 °C for HDPE, 425 °C and 440 °C for PET specimens.

At the end of the TGA test, the PET sample showed an amount of residue approximately equal to 16.8%, attributable to the presence of non-volatile components (fly ash and other contents). The percentage of residue was, instead, negligible in the case of HDPE, i.e. 1.4%.

Fig. 7 shows a thermographic image acquired during the laser irradiation tests. The intense yellow part represents the irradiated area, while the temperature measurement area is present inside the circle. Fig. 4 shows the temperature diagrams as a function of the exposure time of the polymers to radiation. The black HDPE irradiation took place using low power, equal to 10% of the nominal power of the source and caused the appearance of a chromatically altered area. PET is almost totally transparent to laser radiation with an amount of energy transmitted above 90%. As shown in Fig. 8, temperatures above 120 °C were reached during tests, corresponding to about half the melting temperature of the material. A power of 200 W was used, corresponding to 100% of the nominal power of the source, with exposure times of 75 s. In such conditions, the presence of a white halo can be seen, caused by the interaction with the laser beam.

3.2. Tensile test

In Fig. 9, the appearance of the HDPE and PET samples before and after the tensile test can be seen. As shown in the latter, the chromatic alteration of the materials due to laser radiation can be observed. HDPE, with a melting point of about 130 °C, was irradiated at the minimum laser power of 20 W for 20 s (Table 3). Due to the black pigment of the material, the energy was enough to determine a maximum value of surface temperature of 200 °C. On the other hand, PET, which is almost totally transparent to laser radiation in the fixed irradiation conditions (i.e. 200 W for 75 s), reported a maximum temperature of 122 °C, far from the melting temperature of 250 °C.

Fig. 10 shows the stress-strain curves obtained for the HDPE and PET samples and Table 5 shows the comparison of the irradiated materials with respect to the reference (non-irradiated) ones in terms of percentage variations of some tensile parameters. During the tensile test of both

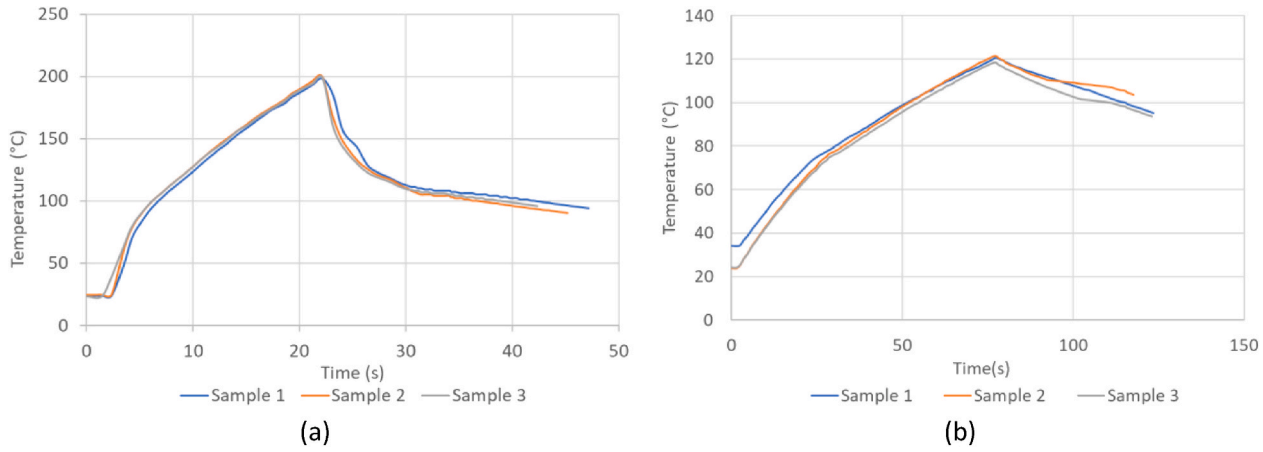

Fig. 8. Temperature-time diagram (relative to exposure to the laser source), for (a) HDPE and (b) PET polymers.

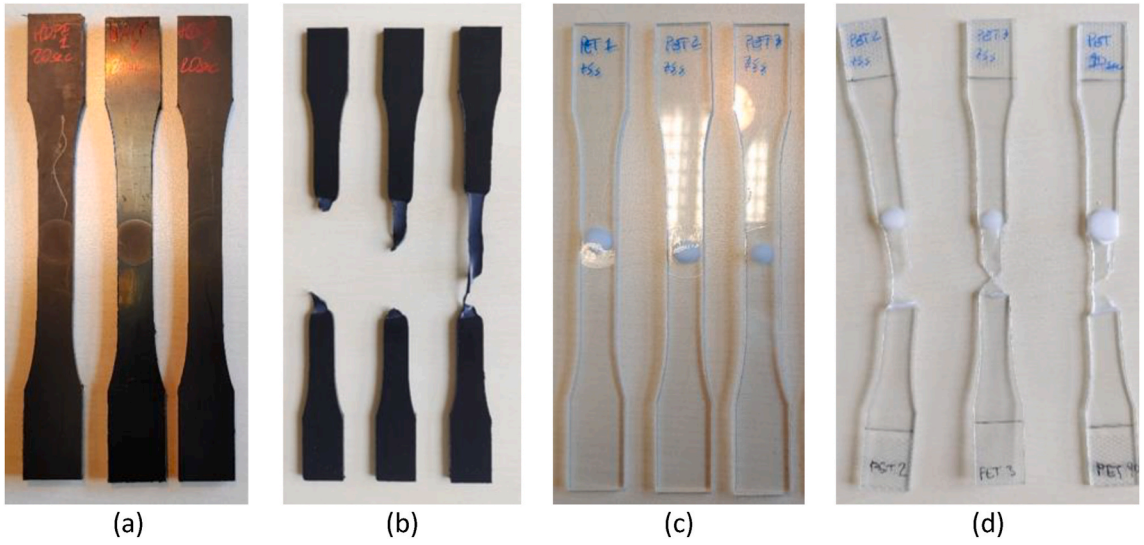

Fig. 9. HDPE (a,b) and PET (c,d) samples after laser irradiation, before (a,c) and after (b,d) the tensile test.

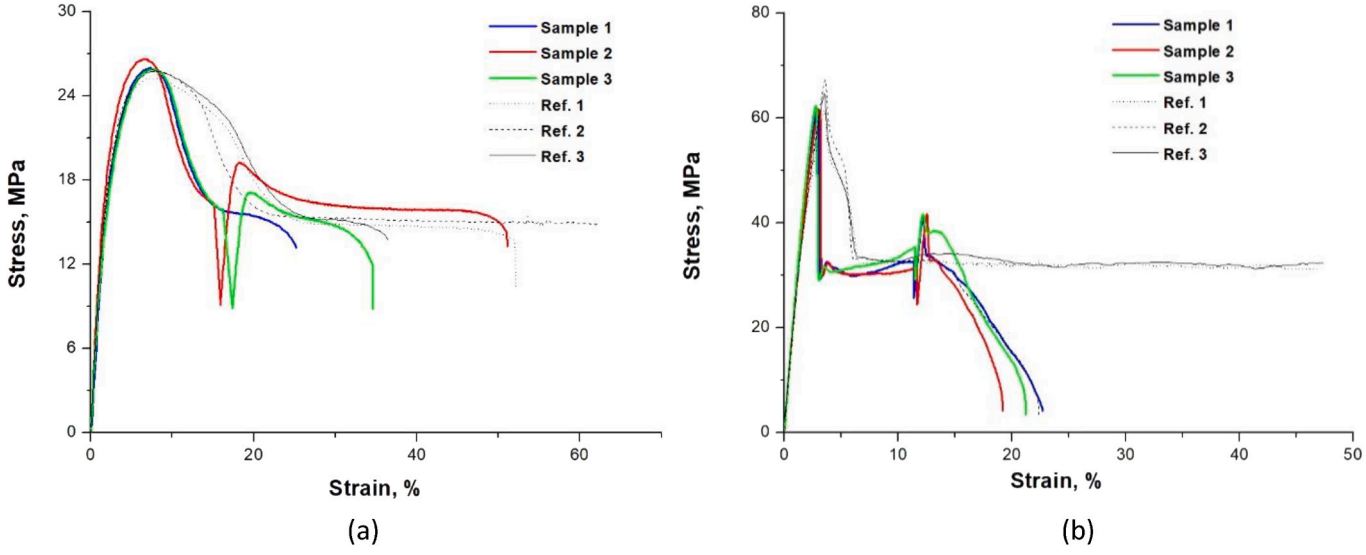

Fig. 10. Stress-strain curves related to irradiated HDPE (a) and PET samples (b).

Table 5
Percentage variation of the tensile mechanical properties of irradiated HDPE and PET, compared to reference materials.

Material	ΔE, %	ΔUTS, %	$\Delta\sigma_R$, %	$\Delta\sigma_S$, %	$\Delta\varepsilon_R$, %
HDPE	+0.9	+1.9	−7.9	−0.1	−26.8
PET	+6.8	−5.8	−82.5	+0.22	−46.0

materials, the formation of a central narrowing area is observed in the irradiated zone, with consequent breakage in the same area. Regarding the effect of the irradiation process on the tensile parameters (Table 5), apart from the elongation at break, which appears to be negatively affected and the strength which does not appear to be significantly altered for both materials, the other parameters (stiffness, resistance to rupture, and UTS) are significantly affected only for PET samples. This consideration, apparently anomalous given that the maximum temperature of the irradiated region is well below the melting temperature of PET, is still under investigation.

3.3. Differential scanning calorimetry

DSC measurements were used to record the changes in the material structure of HDPE and PET caused by irradiation. Fig. 11 shows the diagram obtained and the relative analysis for the determination of the main thermal properties. The data obtained from the DSC before and after irradiation are shown for comparison in Table 6. Following the

Table 6
Thermal properties and percentage of crystallinity evaluated by DSC for HDPE before and after laser treatment.

Cycle	T_m, °C		T_c, °C		X_c, %
Before irradiation					
1st	135.31		112.88	114.82	62.12
2nd	132.90		113.73	115.73	57.20
After irradiation					
1st	131.97	134.63	112.04	116.56	60.17
2nd	130.07	134.60	111.58	116.97	51.57

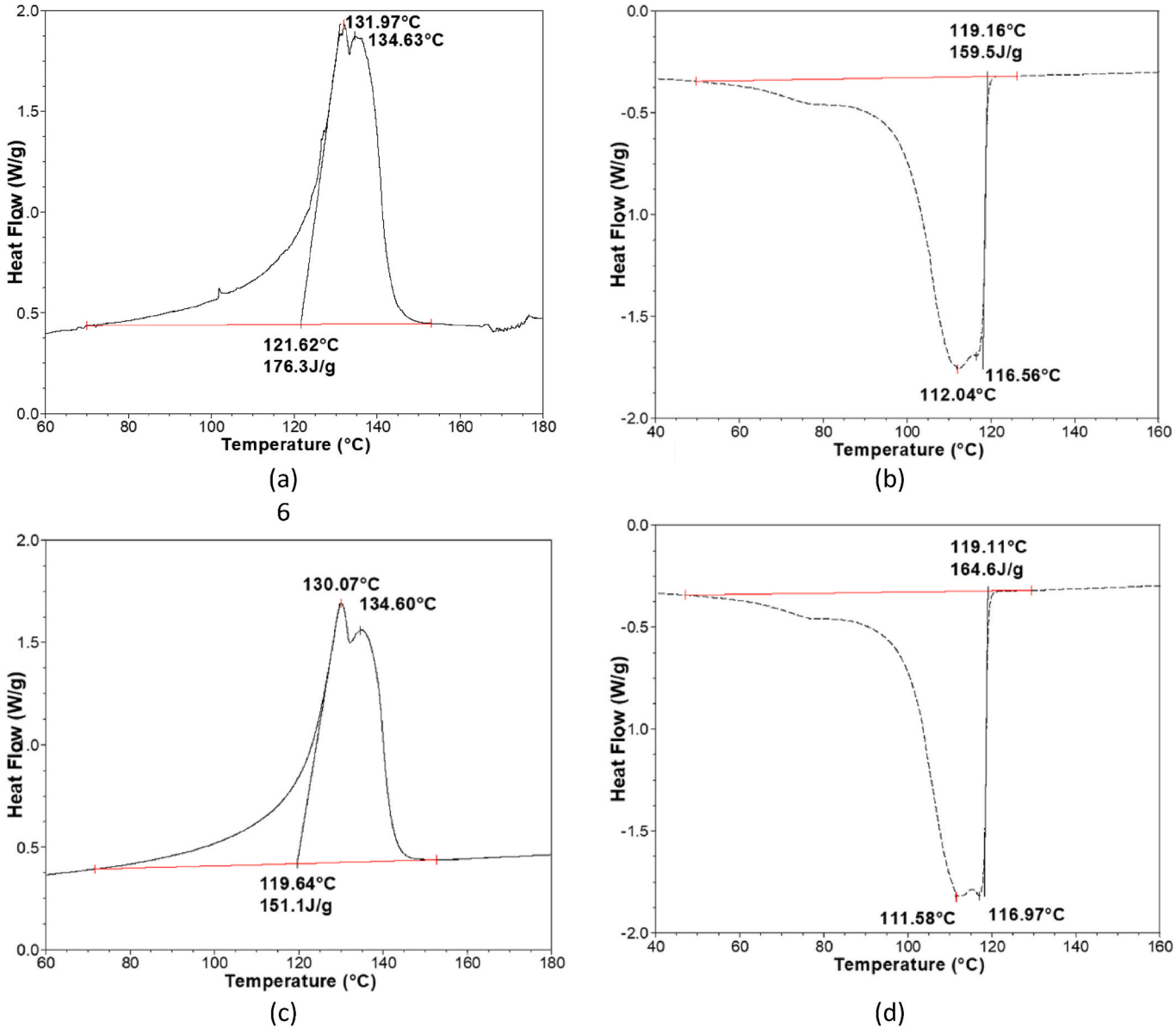

Fig. 11. DSC curve of irradiated HDPE with both heating/cooling cycles: (a,c) evaluation of the melting temperature and enthalpy respectively during the first and second heating cycles; (b,d) evaluation of the crystallization temperature and enthalpy respectively during the first and second cooling cycles.

laser treatment, a splitting of the HDPE melting peak centred at the T_m of 135.3 °C into two peaks, with maximum absorption at about 132.0 °C and 134.6 °C, is observed. Comparing the double crystallization peak before and after the laser treatment, an increase in the separation between the two peaks and, therefore an increase in the difference between the two crystallization temperatures (T_c) is observed. During both heating and cooling cycles, the presence of a double peak in correspondence with the state changes (bimodal trend) and slight discrepancy in T_m and T_c, compared to the reference HDPE, indicates a change of the structure. The occurrence of two crystallization temperatures, even for untreated samples, can be explained by a slight degradation of the sample during its preparation. Because of the high temperatures for polymer processing, degradation occurs related to thermal stress in combination with mechanical stress during the processing inside an extruder and further formation by moulding [39,40]. The changes in polymer chain structure can also be seen through the crystallinity degree, calculated according to Equation (2), whose results are presented in Table 6. Following the laser treatment, a small decrease in the crystalline percentage of HDPE is observed. This could be explained by the higher concentration of formed polymer radicals with different functional groups (carbonyl, carboxyl, hydroxyl, vinyl) because of partial depolymerization induced by exposure to laser conditions. Such groups disable the fine order of polymer chains, and the crystallinity degree decreases [41].

In literature [16], it is known that the crystalline structure, hence the melting behaviour of PE, is governed by two dominating factors: (i) the size of the molecules and (ii) the number of irregular structures. On the one hand, decreasing the size of the molecules facilitates the acquisition of an ordered structure, so favouring an increase in crystallinity and T_m. On the other hand, irregular structures, and end groups within the chains, such as branching points, hydroxyl or carbonyl, tend to decrease the close-packing ability and, therefore also the crystallinity decreases. DSC results highlighted the need to consider cooperative mechanisms in understanding the phenomenon of polymer degradation. A further aspect to consider is that the degradation below the T_m is limited to amorphous phase, which explains why variations in crystalline content are contained following laser treatment [42]. It is worth noting that in the present study treated polymers are commercial, therefore presumably in the presence of antioxidants or other additives capable of increasing the deterioration temperatures of the material. The extent and the modality of deterioration phenomena suffered by the material subjected to laser treatment are influenced by the particles and pigments present (i.e., HDPE is filled with carbon blacks). Carbon black, which is comparable to some of the less effective thermal antioxidants under accelerated test conditions, can provide protection for polyethylene below the melting point. This greater protection in the solid state can be attributed to the impermeability of the crystalline phase to oxygen and to the greater concentration of the voluminous particles of carbon (antioxidant) in the amorphous region [42]. The deterioration mechanism also depends on the cooling rate of the irradiated polymer. On the other hand, the cooling process itself is influenced by the speed and the exposure time of the material to heat, and therefore to the laser source. The use of the laser implies a very intense heating in a very short time, which affects only the most superficial layers of the material. The trend of the degradation of the material will also take into consideration the method of heat diffusion in the underlying layers.

About PET, the average variations of the thermal parameters obtained on three replicates of samples, before and after laser irradiation, were taken into consideration as results. By comparing the first thermal cycles before and after the heat treatment it is possible to obtain an evaluation of the effects determined by the laser on the material. An average T_m of 249.0 ± 0.8 °C was recorded, with a variation of −1.7 °C due to the heat treatment and an average decrease in crystallinity equal to 3%. The average variation of the crystallization temperature following the treatment was negligible. For all PET samples, comparing the first thermal cycles, a T_g was found around 78 °C before irradiation, in any case recording a decrease of about 3 °C of this value in the treated material. The visible transition that occurs around the T_g in PET sample prepared under standard process conditions is the enthalpy relaxation due to physical aging [43]. The cold crystallization peak was therefore detected during the first thermal cycle in both treated and untreated PET by recording an exothermic peak at about 130 °C ($T_{cold\ c}$). As expected, the thermal DSC analysis for this material demonstrated the absence of structural variations and degradation phenomena following the laser treatment under the applied conditions. On the other hand, a slight variation in crystallinity is visible, justified by a slight decrease in temperature following the laser treatment (see Table 7).

3.4. FIMEC indentation test

Fig. 12 reports the typical FIMEC curves found for the samples of HDPE (a) and PET (b), where the applied load is reported as a function of the residual depth.

Moving from the indentation point P1 to the indentation point P10, it is possible to observe a very precise trend, for both materials. In fact, the profile of the curves varies as the test is performed towards the most central positions of the sample (P4–P6) and then resumes the initial trend at the endpoints of indentation. The trend found consistently describes the varying conditions of the polymers passing from point P1 to point P10. In fact, point P1 and point P10 correspond to the untreated material, while in the central positions there is the material that has been irradiated under the laser source.

Fig. 13 compares the load curves obtained for HDPE and PET in the respective P5 positions. For PET, a rather linear increasing trend of the load can be observed at the beginning of penetration, followed by a bend and by an increasing branch of the applied load at higher penetration depth. In comparison, HDPE shows less linearity in the initial section followed by a wide bend and a branch that describes a slow growth of the applied load. The difference in mechanical response for the two materials is evident, as at 0.5 mm of penetration depth HDPE and PET reach respectively 71 N and 177 N.

Many parameters can be extracted from load vs. penetration curves to analyze laser treated materials on a comparative base, such as the load value at fixed penetration depth. In particular, the value of the load reached at 0.5 mm penetration depth was considered. Fig. 14(a) shows how FIMEC test is able to identify variations in the surface of the material as a result of laser radiation. For all positions from P3 to P7, a net decrease in the maximum load applied is observed for PET, i.e. ∼ 14.6%, while the decrease in the mechanical response is more gradual and less relevant for HDPE, i.e. ∼ 7.7%. Fig. 14(b) shows the variation of the resistance parameter P_y as the indentation position varies. The parameter is identified as the specific stress value, corresponding to the real pressure value (P) that separates the first plastic section from the second plastic section and corresponds to the appearance of a permanent macroscopic deformation of the material and to the beginning of the protrusion of the material around the indenter. The test results show a decrease in the P_y parameter at the central positions reached by the laser radiation, of ∼ 37% for PET and ∼ 18.6% for HDPE. In particular, from the analysis of both the maximum loads and P_y parameters, the range of

Table 7
Thermal properties and percentage of crystallinity evaluated by DSC for PET before and after laser treatment (*consider the values as averages measured on three replicates).

Cycle	* T_g, °C	* $T_{cold\ c}$, °C	* T_m, °C	* T_c, °C	X_c, %
Before irradiation					
1st	78.26	130.62	250.70	176.55	21.11
2nd	81.54	–	248.04	175.59	20.98
After irradiation					
1st	75.33	129.76	249.0	176.74	24.03
2nd	80.73	–	245.12	176.27	23.96

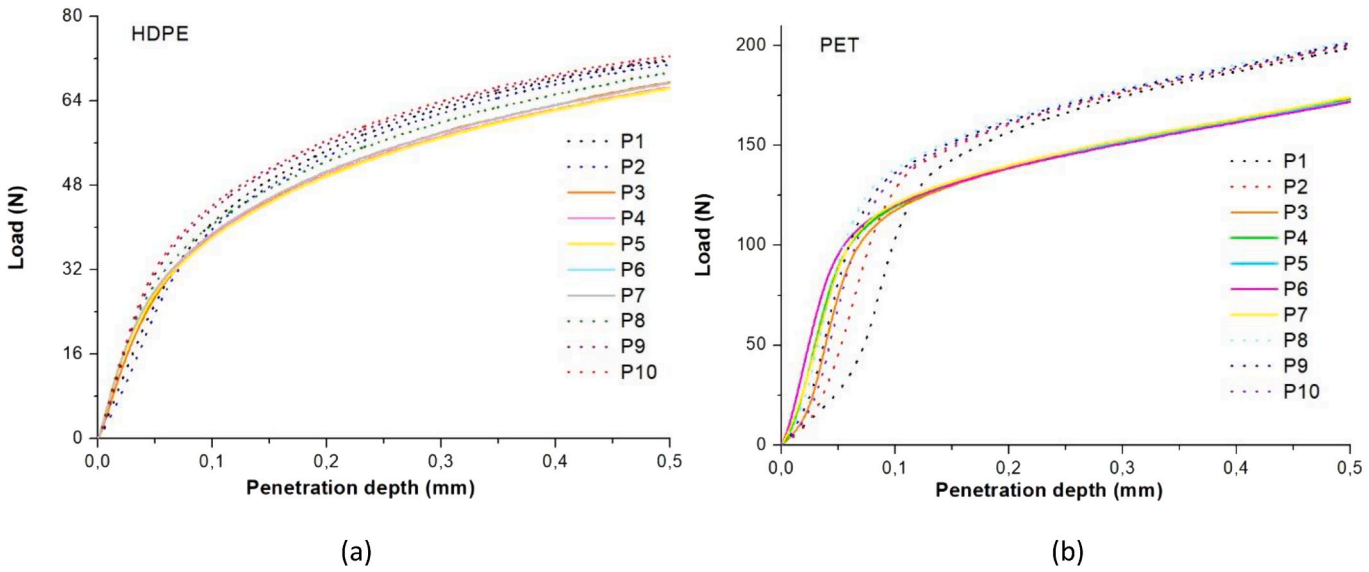

Fig. 12. Results of FIMEC test on HDPE (a) and PET (b).

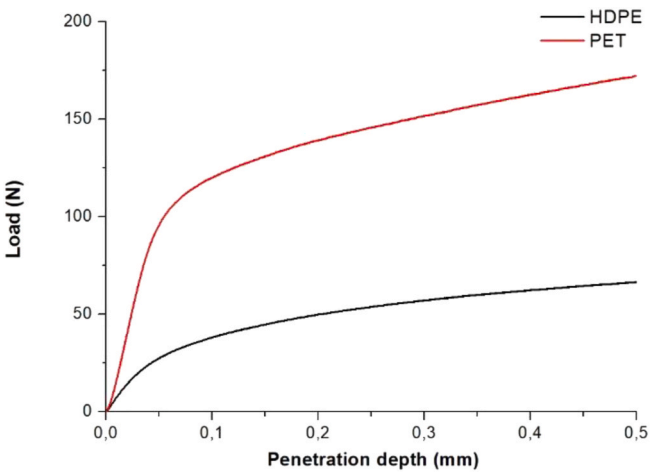

Fig. 13. Results of FIMEC test performed in position P5 on HDPE and PET.

positions P3–P7 appears to be the most influenced by the laser treatment, demonstrating the ability of FIMEC test in detecting the variation in surficial mechanical properties of the materials, after a laser treatment. These tests suggest a decrease in resistance of the material in the central area, so a change in the resistance of the material as a function of both the intensity of the laser beam and the irradiation time.

3.5. Infrared analysis

FTIR spectroscopy can successfully determine any signs of degradation induced on the HDPE surface during laser treatment. In this regard, Fig. 15 shows a comparison of the spectra obtained for the HDPE sample, relative to the irradiated and untreated areas. Table 8 shows the peak identification for the irradiated sample and the reference, i.e. polyethylene.

Characteristic peaks for polyethylene are present at 2912 cm^{-1} and 2850 cm^{-1} assigned to CH stretching in $–CH_2–$ groups. At 1470 cm^{-1} there is a C–H bending band of CH_2 groups, while the signal at 722 cm^{-1} corresponds to the CH_2 rocking mode of the sequence of CH_2 groups in paraffin structure [40].

Following the laser treatment, additional peaks are observed in the HDPE spectrum which are typical of oxidative degradation pathways. The spectrum was compared to library database and found to be consistent with slightly oxidized polyethylene. The spectrum of irradiated HDPE shows a moderate decrease of the intensity of characteristic peaks due to the degradation process. By normalizing all absorptions with respect to the most intense peak of untreated HDPE present around 2912 cm^{-1}, relative to the C–H asymmetric stretch in CH_2, the absorbance of the corresponding signal in the treated HDPE is equal to 0.8. In the HDPE spectrum recorded on the irradiated area, the most resolved band located at 1640 cm^{-1} is visible, which belongs to the vibrational stretching of the carbon double bond (–C═C–). The oxidation effect is also evident from the appearance of the less resolved band (Fig. 15) relating to the stretching vibrations associated with the carbonyl groups of esters and ketones. In fact, it is possible to trace the presence of the carbonyl ester (–COO–) around 1740 cm^{-1} and the absorptions related to the carbonyl ketone (–CO–) at 1715 cm^{-1} [44–46]. A further additional peak can be observed at 909 cm^{-1}, associated with the formation of terminal vinyl groups ($H_2C═C–$), associated with a degradation of HDPE. According to Ref. [16], the relative amount of ketones decreased with heating time, while acids and ester increased. The olefinic groups originally present (i.e. vinylidene, vinyl, and *trans*-vinylidene) disappear gradually with increased heating time.

Degradation of polyethylene in the first step manifests as the chain scission and can be detected through the monitoring of peaks absorbance intensity at 2912 cm^{-1} and 2850 cm^{-1}, assigned to CH stretching in $–CH_2–$ groups. However, as previously discussed, the variation in intensity of these groups is slight following the laser treatment, demonstrating the moderate entity of the oxidative process [44,47].

Polyethylene degradation mostly results with the formation of carbonyl groups (the assigned peak at 1715 cm^{-1}) which are the main result of the thermo- and photo-oxidation of polyethylene. The formation of other groups reported in the literature, such as γ-lactones at 1780 cm^{-1}, hydroperoxides/alcohols at 3420 cm^{-1}, is negligible [40,48] while unsaturation at 910, 965, 990, and 1640 cm^{-1} are still detectable from the spectrum. In any case, carbonyl groups formation is an effective parameter for monitoring the photo-oxidation degree of polyethylene and can be presented as carbonyl index (*CI*), which is given by the ratio between the absorbance of the integrated band of the carbonyl peak and that of the methylene scissor peak (CH_2), calculated according to Equation (3) [49]:

$$CI = \frac{absorption\ at\ 1720\ cm^{-1}}{absorption\ at\ 1462\ cm^{-1}} \quad (3)$$

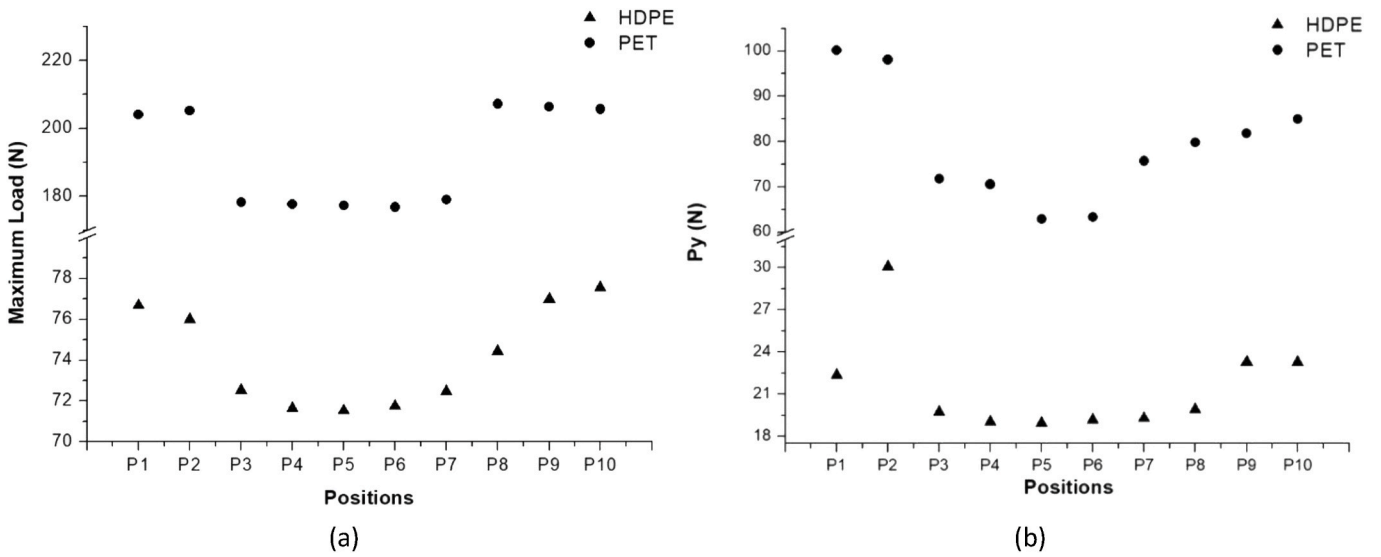

Fig. 14. FIMEC test on irradiated HDPE and PET samples: values of the loads (a) and of the resistance parameters, P_y (b) as a function of the indentation positions (from P1 to P10).

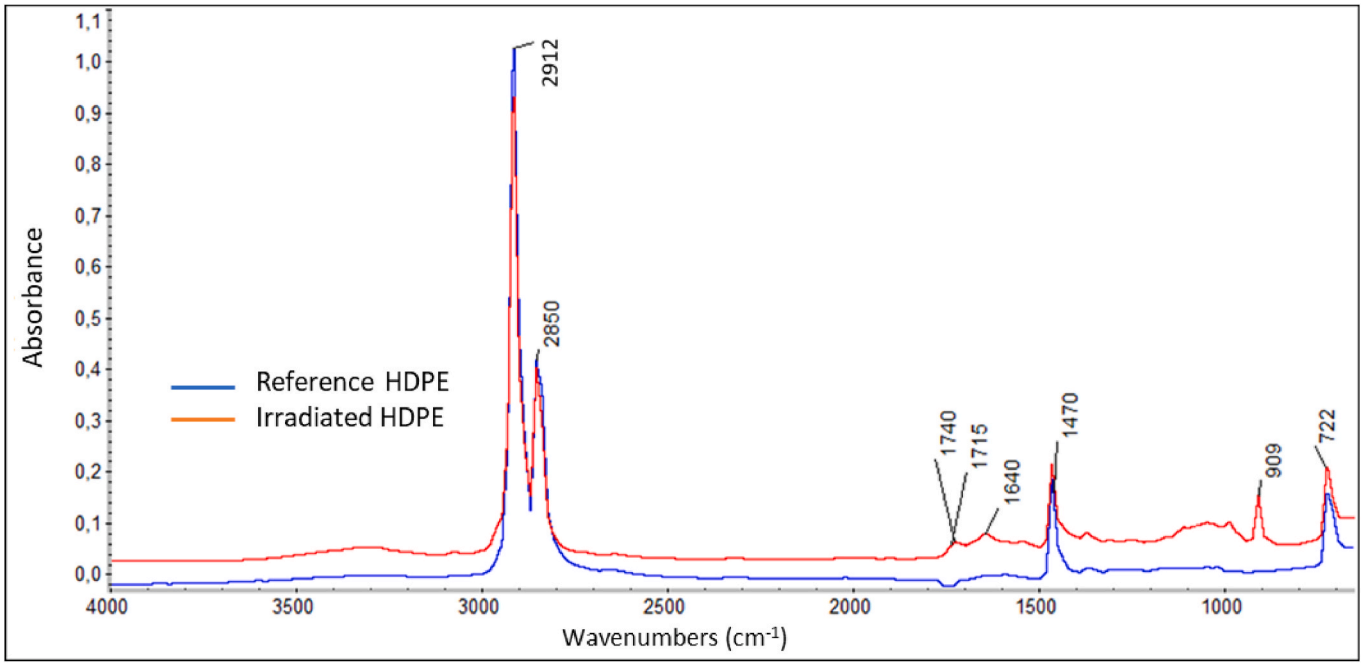

Fig. 15. FTIR analysis: comparison between spectra of reference and 10% irradiated HDPE.

Table 8
Peaks' identification for the reference PE and for the irradiated HDPE.

FTIR Peaks and Identifications		
IR Frequency (cm^{-1})		Functional Groups
Irradiated HDPE	Reference PE	
2912	2912	C–H asymmetric stretch in CH_2
2850	2850	C–H symmetric stretch in CH_2
1740		-COO-
1715		-CO-
1640		-C═C- stretch
1470	1470	CH_2 bend
905–915		H_2C═C-
722	722	CH_2 rock

A higher value of carbonyl index indicates a higher degree of polymer degradation. The carbonyl index value was calculated for HDPE in the irradiated area at 10% using the band composed of several peaks in the range 1764-1685 cm^{-1} resulting in 0.80. As a future objective, this parameter can be useful to monitor the progress of polymer degradation during laser joining operations for the realization of metal-polymer hybrid structures.

About PET, the spectra of this material before and after the treatment are superimposable in the whole range analyzed, except for the area between 2800 cm^{-1} and 3000 cm^{-1}, relative to the stretching vibrations of the C–H bonds (Fig. 16). The slight variation can be charged to some structural rearrangement in terms of crystallinity, due to the laser annealing process.

The decrease in the CH_2 signal with the formation of surfaces with a more compact structure can be considered as the result of a transition

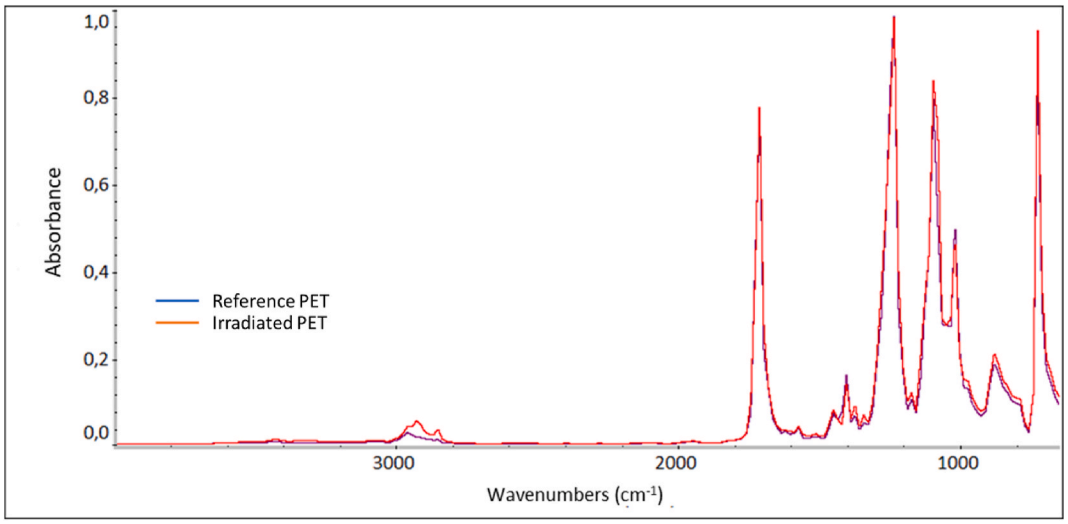

Fig. 16. FTIR analysis: spectrum of the reference PET (blue trace) and of the 50% irradiated PET (red trace). (For interpretation of the references to colour in this figure legend, the reader is referred to the Web version of this article.)

from a liquid-like structure to a more crystalline like structure [50].

Obtained results characterize degradation mostly on the surface of the composite, while the degradation is supposed to be significantly less present in material bulk [40]. At the same time, it should be considered that semi-crystalline polymers tend to disperse the radiation by virtue of the presence of the crystalline phase, generating a greater path length that the radiation must travel before leaving the material and, therefore, a greater absorption along the thickness. Therefore, this factor should also be considered in the evaluation of degradation. In any case, it is worth noting that, due to laser treatment, there is a chromatic alteration of the surface of the samples in the area scanned by laser, which is opaque in the case of HDPE and shinier in the case of PET.

The structural changes undergone by HDPE can be better explained by considering the chemical degradation mechanisms of the polymer. In general, the approaches reported for the analysis of plastic degradation can be grouped into methods associated with the evaluation of the elimination of small molecules, methods that evaluate chemical changes in the polymer structure, related to modifications of functional groups, and methods that record physical changes in the properties of materials (tensile strength, surface morphology, crystallinity, etc.). Chemical methods refer to changes at the molecular level, such as bond splitting or oxidation of long polymer chains to create new molecules, usually with significantly shorter chain lengths. The latter refer to changes in the structure of the mass, such as cracking, embrittlement, and flaking [44].

For PE, since the role of the light in photo-oxidative degradation is only to initiate chain reactions, similar product distributions are generated in both photochemical and thermal processes [44] (Fig. 17). A difference between oxidation by heat and light is that the resulting ketones are stable to heat but not to light. The level of thermal degradation strictly depends on the temperature, with higher values achievable at higher temperatures [51]. Furthermore, the application of mechanical stress can accelerate the degradation of the polymer. In fact, the degradation mechanisms depend on the morphology of the polymer, which can undergo changes because of mechanical stress. It was observed that the influence of mechanical stress can accelerate photo-degradation while the application of mechanical stress alone can cause degradation [51].

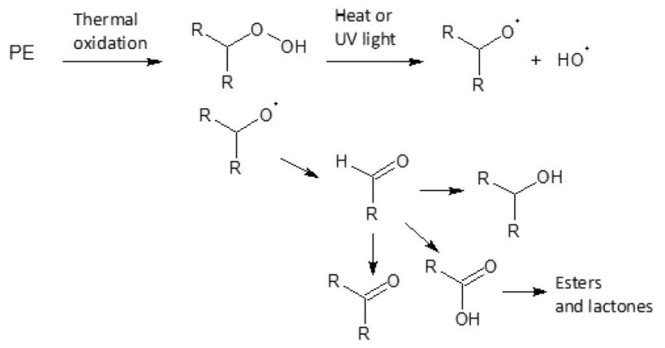

Fig. 17. Common products in the thermal- and photo-oxidative degradation processes for polyethylene. Please note that "R" represents a polymer chain of variable length.

In general, the instability of polyolefins can be attributed to the presence of impurities, such as carbonyl groups or hydroperoxides, that are formed during the manufacturing process of plastics. It is generally known that PE is the most inert of the polyolefins and degrade slowly in the natural environment. The backbone chains of PE, constructed exclusively from C–C single bonds, may also contain a small number of unsaturated (C═C) bonds in the main chain or at the chain ends (typically, vinyl groups in HDPE).

Thermal oxidative degradation of PE does not occur at appreciable rates at temperatures below 100 °C [51].

Fig. 17 illustrates some of the products formed because of the polyethylene degradation process. The oxidation reactions, which are known to occur preferentially close to the sample surface, begin the degradation process of the material [40,52].

The mechanism of photo-oxidative degradation starts when an excited state (localized at a carbonyl or other structural defect) in PE subtracts a hydrogen atom from the polymer backbone, generating a reactive carbon-based alkyl radical. The first step in the subsequent radical chain mechanism is the reaction of the alkyl radical with O_2 to form a peroxy radical, which subtracts a hydrogen atom from another polymer chain (or from a distant site on the same polymer chain) to form a hydroperoxide and a new alkyl radical. The hydroperoxide group (–CH–OOH) which is the product of the primary oxidation is unstable both thermally and photolytically: its decomposing generates a splitting of the O–O bond, forming alkoxy and hydroxyl radicals. Each of these compounds can extract another hydrogen atom and generate a new alkyl radical by participating in a chain reaction, where termination occurs through bimolecular radical recombination [44,52].

Carbonyl defects (ketones) introduced into carbonic skeleton of polyethylene via oxidative reactions can undergo Norrish Type I and/or Norrish type II degradations, responsible for the formation of vinyl groups (Fig. 18) [53]. Although HDPE nominally has the same chemical

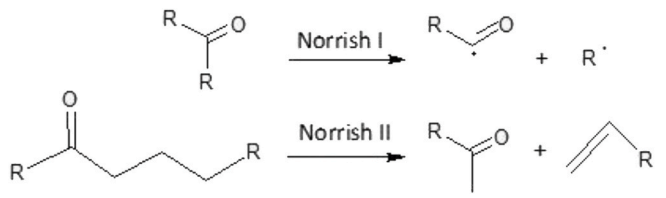

Fig. 18. Norrish type I and Norrish type II mechanisms related to the degradation of polyethylene. Please note that "R" represents a polymer chain of variable length.

composition, compared to LDPE and LLDPE, it has a higher degree of crystallinity. The rate of degradation strongly depends on the amorphous fraction of the polymer. Thus, degradation is far slower for crystalline HDPE, whose lower chain mobility promotes radical recombination at the expense of radical propagation reactions [54]. The presence of carbonyl groups in a degraded polymer indicates that oxidation has taken place and that the vulnerable material can further degrade if these groups are photolabile [55]. Following the analysis of the mechanisms and products of PE thermal degradation, it was possible to establish correlations with the respective absorptions resulting from the FTIR analysis.

4. Conclusions

The study of the degradation processes that affect materials during laser treatment is critical to ensure the quality of this innovative manufacturing technology. With the aim of realizing hybrid metal-polymer junctions, materials are subjected to local melting during laser processing, necessary for the realization of the joint, so to physical and chemical transformations which could affect the quality of the obtained junctions. In this context, the effects of the interaction of a high energy efficiency diode laser beam with two polymers, such as black HDPE and PET, were examined and compared. In the first case, the laser parameters, set at minimum power, i.e. 20 W, determine a partial oxidation of the material during irradiation. Instead, in the second case, despite the higher power, i.e. 200 W, the irradiation is conducted under mild conditions, compared to the critical degradation conditions of the material. TGA technique was exploited to investigate the thermal stability of polymers, to identify the degradation phenomenon, and therefore to select the experimental conditions of laser irradiation for each material investigated.

Tensile tests showed a significant decrease in the strain at break on all irradiated samples, respectively of ∼ 27% for HDPE and of ∼ 46% for PET, for which also the stress at break heavily decreases, i.e. ∼ 82.5%. Comparable results were found following the FIMEC tests, i.e. both materials showed a similar trend in correspondence with the irradiated area of the samples. At the same time, there is a decrease in the maximum loads and in the resistance parameters, which reach the minimum values in the irradiated area. The decrease in maximum loads is ∼ 14.6% and ∼ 7.7%, respectively for PET and HDPE, while the resistance parameters decrease of ∼ 37% for PET and ∼ 18.6% for HDPE.

DSC thermal analysis and FTIR spectroscopy demonstrated the absence of structural variations and degradation phenomena for PET following the laser treatment under the applied conditions, unless a slight reduction in the degree of crystallinity, i.e. 3%. On the other hand, the results of DSC and FTIR analyses on black HDPE highlighted a degradation principle, though the high peak surface temperatures (i.e. 200 °C at 20 W) recorded during irradiation did not determine the occurrence of advanced degradation phenomena. This behaviour can be attributed to a very short processing time for the laser radiation. Specifically, through FTIR analysis it was possible to trace the presence of functional groups, characteristic of the oxidative process of polyethylene, such as carbonyl groups (ketones and esters) and vinyl groups. This result is further confirmed by the DSC analysis showing a shift and resizing of the peaks.

This study allows the definition of the optimal conditions to process HDPE and PET by using a diode laser for the realization of hybrid composite structures without incurring in undesired degradation of the polymers. So, as future study, it is intended to extend the experimental analysis verifying the joining between these polymers and metals by adopting the laser parameters here identified.

Author declaration

We wish to confirm that there are no known conflicts of interest associated with this publication and there has been no significant financial support for this work that could have influenced its outcome.

We confirm that the manuscript has been read and approved by all named authors and that there are no other persons who satisfied the criteria for authorship but are not listed. We further confirm that the order of authors listed in the manuscript has been approved by all of us.

We confirm that we have given due consideration to the protection of intellectual property associated with this work and that there are no impediments to publication, including the timing of publication, with respect to intellectual property. In so doing we confirm that we have followed the regulations of our institutions concerning intellectual property.

We understand that the Corresponding Author is the sole contact for the Editorial process (including Editorial Manager and direct communications with the office). He is responsible for communicating with the other authors about progress, submissions of revisions and final approval of proofs. We confirm that we have provided a current, correct email address which is accessible by the Corresponding Author. For all the authors: Patrizia Moretti.

Declaration of competing interest

The authors declare the following financial interests/personal relationships which may be considered as potential competing interests: Ing. Silvio Genna reports financial support was provided by POR FESR Lazio 2014–2020, Call Gruppi di Ricerca 2020, Project A0375 - 2020–36,716 Laser joIning fOr New hybrid Structures - LIONS - CUP E85F21000820005.

Data availability

Data will be made available on request.

Acknowledgements

This study has been funded through the Programma Operativo Regionale - POR FESR Lazio 2014–2020, Call "Gruppi di Ricerca 2020″, Project A0375 - 2020–36716 ″Laser joIning fOr New hybrid Structures - LIONS" - CUP: E85F21000820005.

References

[1] M.M.A. Kader, G. Jeevi, Recent trends and developments on joints in hybrid composite structures, in: M.S.J. Hashmi (Ed.), Encyclopedia of Materials: Plastics and Polymers, Elsevier, Oxford, 2022, pp. 353–365, https://doi.org/10.1016/B978-0-12-820352-1.00214-5.

[2] Y. Huang, X. Gao, Y. Zhang, B. Ma, Laser joining technology of polymer-metal hybrid structures - a review, J. Manuf. Process. 79 (2022) 934–961, https://doi.org/10.1016/j.jmapro.2022.05.026.

[3] M. Barletta, F. Trovalusci, A. Gisario, S. Venettacci, New ways to the manufacturing of pigmented multi-layer protective coatings, Surf. Coat. Technol. 232 (2013), https://doi.org/10.1016/j.surfcoat.2013.06.113.

[4] Z. Liu, H. Chen, S. Xing, Mechanical performances of metal-polymer sandwich structures with 3D-printed lattice cores subjected to bending load, Arch. Civ. Mech. Eng. 20 (2020) 1–17, https://doi.org/10.1007/s43452-020-00095-1.

[5] M. Sciences, C. Engineer, P. Degradation, S.A. Agent, G. Wypych, Polymer Stability, 2020.

[6] F. Rizzo, F. Pinto, M. Meo, Development of multifunctional hybrid metal/carbon composite structures, Compos. Struct. 222 (2019), 110907, https://doi.org/10.1016/j.compstruct.2019.110907.

[7] F. Lambiase, S.I. Scipioni, C.J. Lee, D.C. Ko, F. Liu, A state-of-the-art review on advanced joining processes for metal-composite and metal-polymer hybrid structures, Materials 14 (2021), https://doi.org/10.3390/ma14081890.

[8] N. Mazlan, T.C. Hua, N. Ramli, K. Abdan, M.H. Zin, Thermoplastics for aircraft cabin applications, in: M.S.J. Hashmi (Ed.), Encyclopedia of Materials: Plastics and Polymers, Elsevier, Oxford, 2022, pp. 482–497, https://doi.org/10.1016/B978-0-12-820352-1.00101-2.

[9] R. Melentiev, A. Yudhanto, R. Tao, T. Vuchkov, G. Lubineau, Metallization of polymers and composites: state-of-the-art approaches, Mater. Des. 221 (2022), 110958, https://doi.org/10.1016/j.matdes.2022.110958.

[10] V.P. Mahesh, S. Patel, A. Gumaste, A. Arora, Joining of polymer matrix composites through friction stir processes, in: D. Brabazon (Ed.), Encyclopedia of Materials: Composites, Elsevier, Oxford, 2021, pp. 352–379, https://doi.org/10.1016/B978-0-12-819724-0.00063-X.

[11] A. Pramanik, A.K. Basak, Y. Dong, P.K. Sarker, M.S. Uddin, G. Littlefair, A.R. Dixit, S. Chattopadhyaya, Joining of carbon fibre reinforced polymer (CFRP) composites and aluminium alloys – a review, Compos Part A Appl Sci Manuf 101 (2017) 1–29, https://doi.org/10.1016/j.compositesa.2017.06.007.

[12] V. Valasamudram, K. Sairam, R. Dinesh Gopal, K. Sridhar, Study and evaluation of cold joining on metals and non metals combinations (ss, al, acr) using polymer based adhesive, Mater. Today Proc. 27 (2020) 2806–2810, https://doi.org/10.1016/j.matpr.2019.12.371.

[13] A. Galińska, Mechanical joining of fibre reinforced polymer composites to metals—a review. Part i: bolted joining, Polymers 12 (2020) 1–48, https://doi.org/10.3390/polym12102252.

[14] M. Schmid, K. Wegener, Additive Manufacturing: polymers applicable for laser sintering (LS), in: Procedia Eng, Elsevier Ltd, 2016, pp. 457–464, https://doi.org/10.1016/j.proeng.2016.06.692.

[15] L. Reich, Salvatore S. Stivala, Autoxidation of Hydrocarbons and Polyolefins, 1969.

[16] A. Holmström, E.M. Sörvik, Thermooxidative degradation of polyethylene. I and II. Structural changes occurring in low-density polyethylene, high-density polyethylene, and tetratetracontane heated in air, J. Polym. Sci. Polym. Chem. Ed. 16 (1978) 2555–2586, https://doi.org/10.1002/pol.1978.170161012.

[17] R. Yang, Chapter 7 - polymer degradation and stability, in: R. Narain (Ed.), Polymer Science and Nanotechnology, Elsevier, 2020, pp. 125–148, https://doi.org/10.1016/B978-0-12-816806-6.00007-8.

[18] M. Kaykhaii, M.R. Linford, International Journal of New Chemistry Characterization of polymeric materials and their degradation products, (n.d.). http://www.ijnc.ir/.

[19] B. Riccardi, R. Montanari, Indentation of metals by a flat-ended cylindrical punch, Mater. Sci. Eng., A 381 (2004) 281–291, https://doi.org/10.1016/j.msea.2004.04.041.

[20] S.E. Arevalo, D.M. Ebenstein, L.A. Pruitt, A methodological framework for nanomechanical characterization of soft biomaterials and polymers, J. Mech. Behav. Biomed. Mater. 134 (2022), 105384, https://doi.org/10.1016/j.jmbbm.2022.105384.

[21] F. Ania, M.A. Gómez-Fatou, H.J. Salavagione, P. Enrique-Jiménez, S. Quiles-Díaz, A. Flores, Creep behaviour of elastomeric nanocomposites by flat punch indentation: influence of graphene modification and content, Compos. Sci. Technol. 198 (2020), https://doi.org/10.1016/j.compscitech.2020.108311.

[22] F. Trovalusci, N. Ucciardello, G. Baiocco, F. Tagliaferri, Neural network approach to quality monitoring of injection molding of photoluminescent polymers, Appl. Phys. Mater. Sci. Process 125 (2019), https://doi.org/10.1007/s00339-019-3067-x.

[23] M. Barletta, M. Puopolo, F. Trovalusci, S. Vesco, High-Density Poly(Ethylene) (HDPE)/SrAl 2 O 4 :Eu 2+ , Dy 3+ Photoluminescent Pigments: Material Design, Melt Processing and Characterization, n.d..

[24] F. Trovalusci, A. Donno, V. Tagliaferri, Statistical analysis of the mechanical properties of injection molded photoluminescent polymers, in: International Conference on Numerical Analysis and Applied Mathematics 2014, 2015.

[25] S. Genna, F. Trovalusci, V. Tagliaferri, Indentation test to study the moisture absorption effect on CFRP composite, Compos. B Eng. 124 (2017) 1–8, https://doi.org/10.1016/J.COMPOSITESB.2017.05.053.

[26] L. Cheng, X. Xia, W. Yu, L.E. Scriven, W.W. Gerberich, Flat-punch indentation of viscoelastic material, J. Polym. Sci. B Polym. Phys. 38 (2000) 10–22, https://doi.org/10.1002/(SICI)1099-0488(20000101)38:1<10::AID-POLB2>3.0.CO;2-6.

[27] S. Yang, Y.W. Zhang, K. Zeng, Analysis of nanoindentation creep for polymeric materials, J. Appl. Phys. 95 (2004) 3655, https://doi.org/10.1063/1.1651341.

[28] A.K. Kalkar, V.D. Deshpande, B.S. Vatsaraj, Isoconversional kinetic analysis of DSC data on nonisothermal crystallization: estimation of Hoffman-Lauritzen parameters and thermal transitions in PET/MMT nanocomposites, Polymer (Guildf). 55 (2014) 6948–6959, https://doi.org/10.1016/j.polymer.2014.10.068.

[29] P. Lewis, C. Gagg, Forensic Polymer Engineering: Why Polymer Products Fail in Service, Woodhead Publishing Limited, 2010.

[30] K. Sharma, O. Braun, S. Tritsch, R. Muff, R. Hufenus, E. Perret, 2D Raman, ATR-FTIR, WAXD, SAXS and DSC data of PET mono- and PET/PA6 bicomponent filaments, Data Brief 38 (2021), 107416, https://doi.org/10.1016/j.dib.2021.107416.

[31] B. Rittenhouse, X. Mi, C. Allen, Beginner's Guide to Twitter Data, Programming Historian, 2019, https://doi.org/10.46430/phen0083.

[32] P. Gijsman, G. Meijers, G. Vitarelli, Comparison of the UV-degradation chemistry of polypropylene, polyethylene, polyamide 6 and polybutylene terephthalate, Polym. Degrad. Stabil. 65 (1999) 433–441, https://doi.org/10.1016/S0141-3910(99)00033-6.

[33] A. Ashraf, A. al Ashraf, Thermal analysis of polymers (LDPE, HDPE) by differential scanning calorimetry technique thermal analysis of polymers (LDPE, HDPE) by differential scanning calorimetry (DSC) technique thermal analysis of polymers by differential scanning calorimetry (DSC) technique introduction. https://doi.org/10.13140/2.1.1558.0963, 2015.

[34] I.I. Salakhov, N.M. Shaidullin, A.E. Chalykh, M.A. Matsko, A. v Shapagin, A. Z. Batyrshin, G.A. Shandryuk, I.E. Nifant'ev, A.M. Korsunsky, Low-temperature mechanical properties of high-density and low-density polyethylene and their blends. https://doi.org/10.3390/polym13111821, 2021.

[35] C. Mittermeier, A. Lion, Challenges in the experimental investigation of the caloric and thermomechanical behaviour of semi-crystalline polymers: a study on the example of polyethylene terephthalate (PET), Polym. Test. 81 (2020), 106252, https://doi.org/10.1016/J.POLYMERTESTING.2019.106252.

[36] A. Anis, A. Yagoub Elnour, M.A. Alam, S.M. Al-Zahrani, F. Alfayez, Z. Bashir, Aluminum-Filled Amorphous-PET, a Composite Showing Simultaneous Increase in Modulus and Impact Resistance, (n.d.). https://doi.org/10.3390/polym12092038.

[37] Y. Kong, J.N. Hay, The measurement of the crystallinity of polymers by DSC, Polymer (Guildf) 43 (2002) 3873–3878, https://doi.org/10.1016/S0032-3861(02)00235-5.

[38] R.L. Blaine, THERMAL APPLICATIONS NOTE Polymer Heats of Fusion, USA, n.d.

[39] I.A. Hussein, K. Ho, S.K. Goyal, E. Karbashewski, M.C. Williams, Thermomechanical Degradation in the Preparation of Polyethylene Blends, n.d.

[40] L.K. Krehula, Z. Katančić, A.P. Siročić, Z. Hrnjak-Murgić, Weathering of high-density polyethylene-wood plastic composites, J. Wood Chem. Technol. 34 (2014) 39–54, https://doi.org/10.1080/02773813.2013.827209.

[41] M. Pracella, L. Rolla, D. Chionna, A. Galeski, Compatibilization and Properties of Poly(ethylene terephthalate)/Polyethylene Blends Based on Recycled Materials, n. d.

[42] W.L. Hawkins, W. Matreyek, F.H. Winslow, The Morphology of Semicrystalline Polymers. Part I. The Effect of Temperature on the Oxidation of Polyolefins, 1959.

[43] B.G. Girija, R.R.N. Sailaja, G. Madras, Thermal degradation and mechanical properties of PET blends, Polym. Degrad. Stabil. 90 (2005) 147–153, https://doi.org/10.1016/j.polymdegradstab.2005.03.003.

[44] A. Chamas, H. Moon, J. Zheng, Y. Qiu, T. Tabassum, J.H. Jang, M. Abu-Omar, S. L. Scott, S. Suh, Degradation rates of plastics in the environment, ACS Sustain. Chem. Eng. 8 (2020) 3494–3511, https://doi.org/10.1021/acssuschemeng.9b06635.

[45] A. Moldovan, S. Paachia, R. Buican, M.H. Ierean, CHARACTERIZATION OF POLYOLEFINS WASTES BY FTIR SPECTROSCOPY, 2012.

[46] A. Ammala, S. Bateman, K. Dean, E. Petinakis, P. Sangwan, S. Wong, Q. Yuan, L. Yu, C. Patrick, K.H. Leong, An overview of degradable and biodegradable polyolefins, Prog. Polym. Sci. 36 (2011) 1015–1049, https://doi.org/10.1016/j.progpolymsci.2010.12.002.

[47] T. Ojeda, A. Freitas, K. Birck, E. Dalmolin, R. Jacques, F. Bento, F. Camargo, Degradability of linear polyolefins under natural weathering, Polym. Degrad. Stabil. 96 (2011) 703–707, https://doi.org/10.1016/J.POLYMDEGRADSTAB.2010.12.004.

[48] S. Morlat-Therias, E. Fanton, J.L. Gardette, N.T. Dintcheva, F.P. la Mantia, V. Malatesta, Photochemical stabilization of linear low-density polyethylene/clay nanocomposites: towards durable nanocomposites, Polym. Degrad. Stabil. 93 (2008) 1776–1780, https://doi.org/10.1016/j.polymdegradstab.2008.07.031.

[49] P.K. Roy, P. Surekha, C. Rajagopal, S.N. Chatterjee, V. Choudhary, Studies on the photo-oxidative degradation of LDPE films in the presence of oxidized polyethylene, Polym. Degrad. Stabil. 92 (2007) 1151–1160, https://doi.org/10.1016/j.polymdegradstab.2007.01.010.

[50] S. Chen, F. Yu, Q. Yu, Y. He, S. Jiang, Strong resistance of a thin crystalline layer of balanced charged groups to protein adsorption, Langmuir 22 (2006) 8186–8191, https://doi.org/10.1021/la061012m.

[51] M. Gardette, A. Perthue, J.-L. Gardette, T. Janecska, E. Földes, B. Pukánszky, S. Therias, Photo- and thermal-oxidation of polyethylene: comparison of mechanisms and influence of unsaturation content, Polym. Degrad. Stabil. 98 (2013) 2383–2390, https://doi.org/10.1016/j.polymdegradstab.2013.07.017.

[52] B. Gewert, M.M. Plassmann, M. MacLeod, Pathways for degradation of plastic polymers floating in the marine environment, Environ. Sci.: Process. Impacts 17 (2015) 1513–1521, https://doi.org/10.1039/C5EM00207A.

[53] R.G.W. Norrish, C.H. Bamford, Photo-decomposition of aldehydes and ketones, Nature 140 (1937), 145–145.

[54] J.M. Restrepo-Flórez, A. Bassi, M.R. Thompson, Microbial degradation and deterioration of polyethylene - a review, Int. Biodeterior. Biodegrad. 88 (2014) 83–90, https://doi.org/10.1016/j.ibiod.2013.12.014.

[55] D. Feldman, Polymer weathering: photo-oxidation, J. Polym. Environ. 10 (2002), https://doi.org/10.1023/A:1021148205366.